Bioorg. Med. Chem. Lett. 40 (2021) 127929

Contents lists available at ScienceDirect

Bioorganic & Medicinal Chemistry Letters

journal homepage: www.elsevier.com/locate/bmcl

Trehalose-based neuroprotective autophagy inducers

Giulia Assoni [a,e], Giulia Frapporti [a,e], Eleonora Colombo [b], Davide Gornati [b,f], Maria Dolores Perez-Carrion [c], Laura Polito [d], Pierfausto Seneci [b,*], Giovanni Piccoli [a,*], Daniela Arosio [d,*]

[a] Department of Cellular, Computational And Integrative Biology, (CIBIO), Via Sommarive 9, I-38123 Povo, TN, Italy
[b] Chemistry Department, Università Statale di Milano, Via Golgi 19, I-20133 Milan, Italy
[c] Unidad Asociada Neurodeath, Departamento de Ciencias Médicas, Universidad de Castilla-La Mancha, Albacete, Spain
[d] Istituto di Scienze e Tecnologie Chimiche (SCITEC) "Giulio Natta", Consiglio Nazionale delle Ricerche (CNR), Via C. Golgi 19, I-20133 Milan, Italy and Via G. Fantoli 16/15, I-20138 Milan, Italy

ARTICLE INFO

Keywords:
Trehalose
Neurodegeneration
Autophagy
Chemical probes
Nanoparticles
Prodrugs

ABSTRACT

A small set of trehalose-centered putative autophagy inducers was rationally designed and synthesized, with the aim to identify more potent and bioavailable autophagy inducers than free trehalose, and to acquire information about their molecular mechanism of action. Several robust, high yield routes to key trehalose intermediates and small molecule prodrugs (**2**–**5**), putative probes (**6**–**10**) and inorganic nanovectors (**12a** – thiol-PEG-triazole-trehalose constructs **11**) were successfully executed, and compounds were tested for their autophagy-inducing properties. While small molecules **2**–**11** showed no pro-autophagic behavior at sub-millimolar concentrations, trehalose-bearing PEG-AuNPs **12a** caused measurable autophagy induction at an estimated 40 μM trehalose concentration without any significant toxicity at the same concentration.

α,α-Trehalose **1** (trehalose from now on, Fig. 1) is a non-reducing disaccharide formed by a 1,1 linkage (refractory to glucosidase cleavage) between two D-glucose molecules[1]. It is widely bio-synthesized in the biological world, but absent in mammals[2]. In extremophile organisms it stabilizes life processes in extreme conditions (freezing or dehydration[3], surviving heat and desiccation stress[4]. It is used in food processing and cosmetics[5], and for the reduction of misfolding of pathologic, aggregated proteins[6].

Due to its high hydrophilicity, trehalose poorly permeates biological membranes. It is not naturally occurring in higher vertebrates, which express on their intestinal membrane trehalases[7] to hydrolyze trehalose in two molecules of glucose, preventing its oral administration. Thus, extremely high dosages are needed for in vivo effects.

Robust *in vitro* evidence show that trehalose induces autophagy at ≥100 mM (Fig. 2)[8]. Mechanistic hypotheses include blocking glucose transporters at the plasma membrane (GLUT) to stimulate autophagy[9], and inducing autophagy *via* transient transcription factor EB (TFEB)-mediated lysosomal enlargement and membrane permeabilization[10].

Trehalose underwent synthetic[11] and biosynthetic transformations[12]. Its regioselective functionalization led to biologically active small molecules (hits, leads[13–14] and chemical probes[15–16]), to glycoclusters[17–18] and to trehalose-based nanoparticles[19].

This study aimed to develop some robust, high yield routes to key trehalose intermediates and small molecule prodrugs (**2**–**5**, Fig. 3), putative probes (**6**–**10**) and inorganic nanovectors (**12a** – thiol-PEG-triazole-trehalose constructs **11**) to be tested for their autophagy-inducing properties, bioavailability and molecular mechanism of action.

The strategy followed to prepare acetylated trehalose derivatives **2**–**5** – using published procedures, often optimizing them in terms of yields, sometimes introducing major changes - is reported in Appendix A – Supplementary Material. Acetylated trehalose derivatives **2**–**5** were submitted to biology profiling as putative autophagy inducers.

6-Azido trehalose **6**[12] and 6,6′-bisazido trehalose **7**[20] were previously synthesized. Rather than reproducing such synthetic routes, we envisaged and successfully assessed a single synthetic strategy which led us to both synthetic targets. Such strategy is shown in Scheme 1. Namely, we submitted trehalose to bromination with 2 equivalents of NBS (step a), then we per-acetylated the crude (step b, Scheme 1). Mono- and bis-

* Corresponding authors.
E-mail addresses: pierfausto.seneci@unimi.it (P. Seneci), giovanni.piccoli@unitn.it (G. Piccoli), daniela.arosio@scitec.cnr.it (D. Arosio).
[e] These authors contributed equally to this project.
[f] Current address: Procos, SpA, via G. Matteotti 249, I-28602 Cameri (NO), Italy.

https://doi.org/10.1016/j.bmcl.2021.127929
Received 30 October 2020; Received in revised form 25 February 2021; Accepted 27 February 2021
Available online 9 March 2021

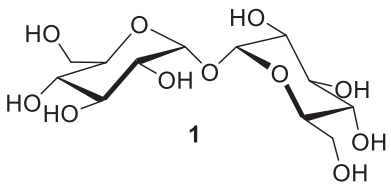

Fig. 1. α,α-Trehalose **1**: chemical structure.

brominated, per-acetylated trehaloses **13** and **14** were obtained in moderate yields, and separated by chromatography. Their substitution with sodium azide and deacetylation in controlled conditions (steps c and d, Scheme 1) led to 6-azido trehalose **6** and 6,6′-bis-azidotrehalose **7** in good yields. Both were submitted to biology profiling as putative autophagy inducers.

Four trehalose monoazides were recently reported, by replacing each hydroxy group of a glucose ring with an azide[12]. We did introduce the azide group on one or both primary hydroxyls in trehalose (compounds **6** and **7**), but we felt that the insertion of a small linker between trehalose and each azide on secondary hydroxyls could preserve its properties, while making an azide more accessible for further derivatization. Thus, we targeted 2- and 4-(5-azidopentyl) trehalose **8** and **9**.

As to the former, its synthesis entailed the introduction of acetals on positions 4 and 6 and per-silylation (step a, Scheme 2), followed by a one pot desilylation – 3-benzylation reaction[21] (step b). Benzylation with sub-stoichiometric benzyl bromide (step c) produced, after chromatography, desired tri-benzyloxy, mono-2-hydroxy trehalose **19** in moderate yields. Its transformation into target 2-(5-azidopentyl) trehalose **8** in good yields entailed alkylation with a large excess of dibromopentane, hydrogenolytic deprotection, peracetylation, azide substitution and careful deacetylation (steps d to h, Scheme 2). Compound **8** was submitted to biology profiling as a putative autophagy inducer.

Trehalose was transformed into its mono-acetal using a 1:1 reagent ratio followed by per-benzylation (steps a and b, Scheme 3) to yield compound **23**. Regioselective acetal opening (step c) was followed by a nucleophilic substitution with a large excess of dibromopentane (step d), a protecting group switch from benzyl to acetyl (steps e, f), an azide substitution (step g), and a carefully controlled deacetylation (step h, Scheme 3). Target 4-(5-azidopentyl) trehalose **9** was obtained in moderate, unoptimized yields and was submitted to biology profiling as a putative autophagy inducer.

Due to the easier synthetic accessibility in larger amounts of 6-azido trehalose **6** when compared to azides **7** to **9**, we used the former as a key intermediate to be converted either into a chemical probe for mechanistic studies, and into constructs for nanovector preparation. Per-acetylated 6-azido trehalose **16** was reacted with *N*-(prop-2-yn-1-yl) biotinamide **28** in a click chemistry protocol (step a, Scheme 4), yielding a per-acetylated, triazole-connected biotin-trehalose adduct in excellent yields. Deacetylation (step b, Scheme 4) led in excellent yields to pure target probe **10**, which was submitted to biology profiling as a putative autophagy inducer.

Gold nanoparticles are reliable theranostics tools, providing benefits in terms of drug delivery[22], photothermal and microwave therapies[23]. Their surface functionalization with biologically active compounds is quite developed[24].

Our efforts towards adduct **11** are depicted in Scheme 5. *t*-Butyl protected PEG alcohol **30** was converted into protected thiol **31**, C-deprotected (**32**) and amidated with propargylamine (**33**, steps a-c, Scheme 5) in standard conditions with excellent yields. Then, linker **33** was conjugated through copper-catalyzed Huisgen cycloaddition with acetylated 6-azido trehalose **15** to give PEG-triazole trehalose conjugate **34** in good yields (step d). Deacetylation (step e, Scheme 5) in standard conditions led to excellent yields of sufficiently pure target adduct **11**; the presence of disulfide-connected dimer **35** does not affect AuNPs' preparation because it should be reduced *in situ* by $NaBH_4$ (*vide infra*).

Trehalose-bearing AuNPs **12a** were prepared by reduction of tetrachloroauric acid by $NaBH_4$ in presence of the thiol-PEG-triazole trehalose conjugate **11**, using a reported procedure[25]. The resulting dark suspension of AuNPs was shaken for ca. 2 h at RT, and purified by centrifugal filtration. AuNPs **12a** were water-soluble and could be re-dissolved after lyophilization. TEM analysis showed that trehalose-functionalized AuNPs **12a** were characterized by a very small core (ca. 4.6 nm) and were almost uniformly dispersed, without signs of aggregation (see Supplementary Material).

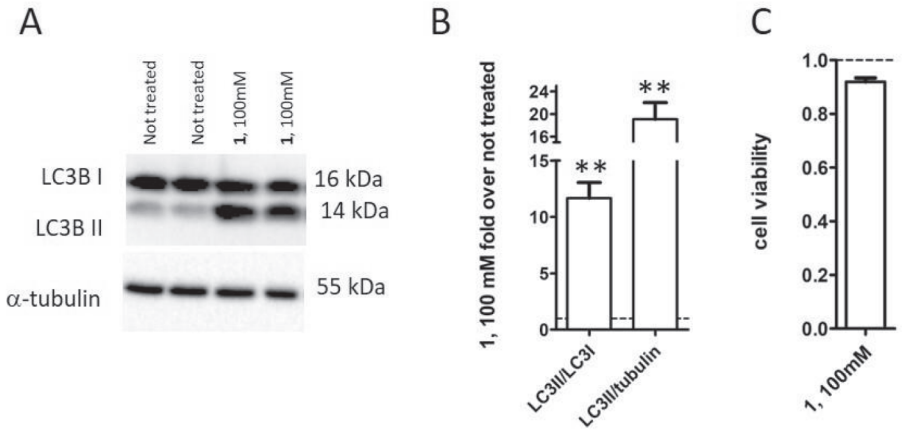

Fig. 2. Autophagy induction and cytotoxicity assays on compound **1** upon 24 h treatment (A). Graphs report LC3BII/LC3BI ratio and LC3BII amount expressed as fold over α-tubulin (B), and cell viability. Each value was normalized on not treated control, set at 1. Data are expressed as mean ± S.E.; n = 6–8, ** $p < 0.01$.

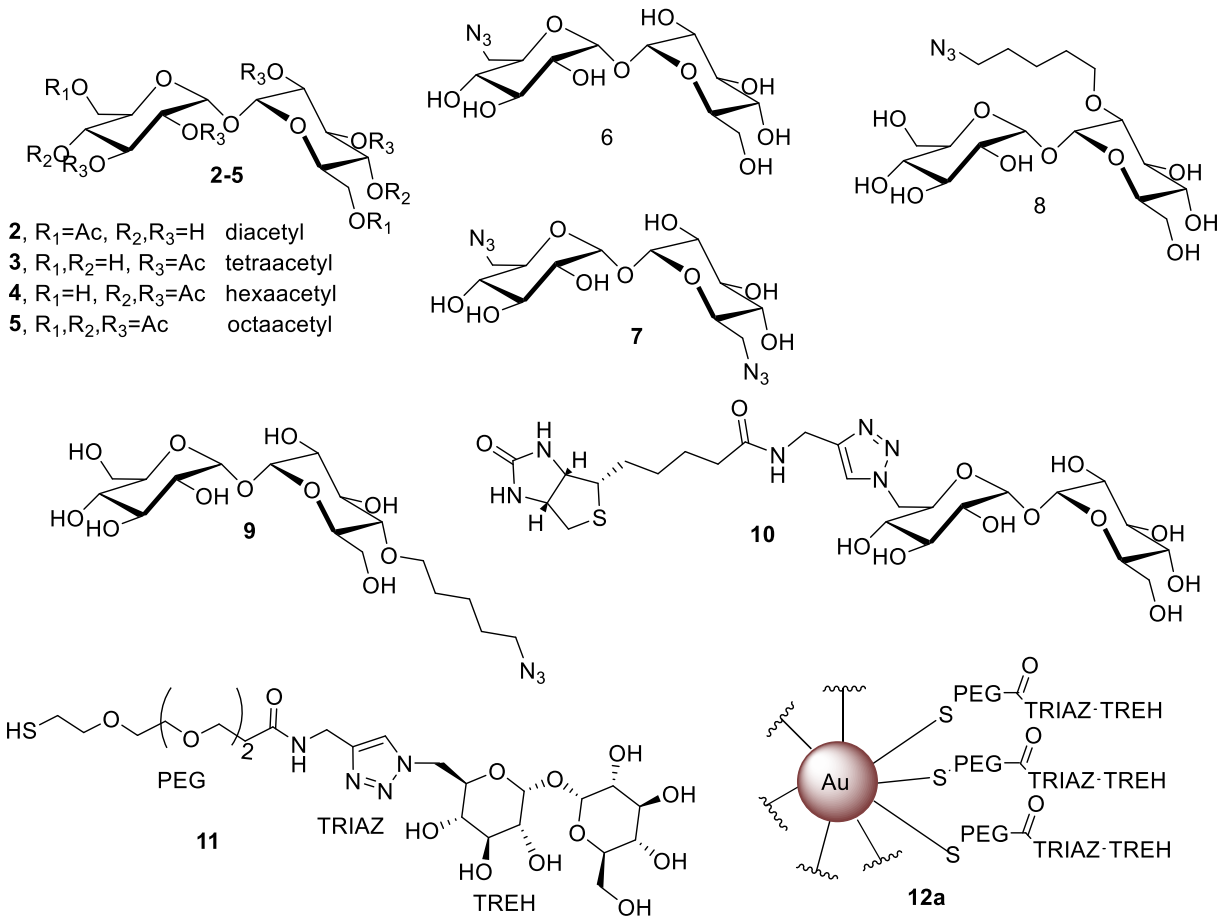

Fig. 3. Targeted trehalose modifications: putative prodrugs (**2**–**5**), analogues (**6**–**9**), chemical probes (**10**), trehalose-linker constructs (**11**) and trehalose-based nanovectors (**12a**).

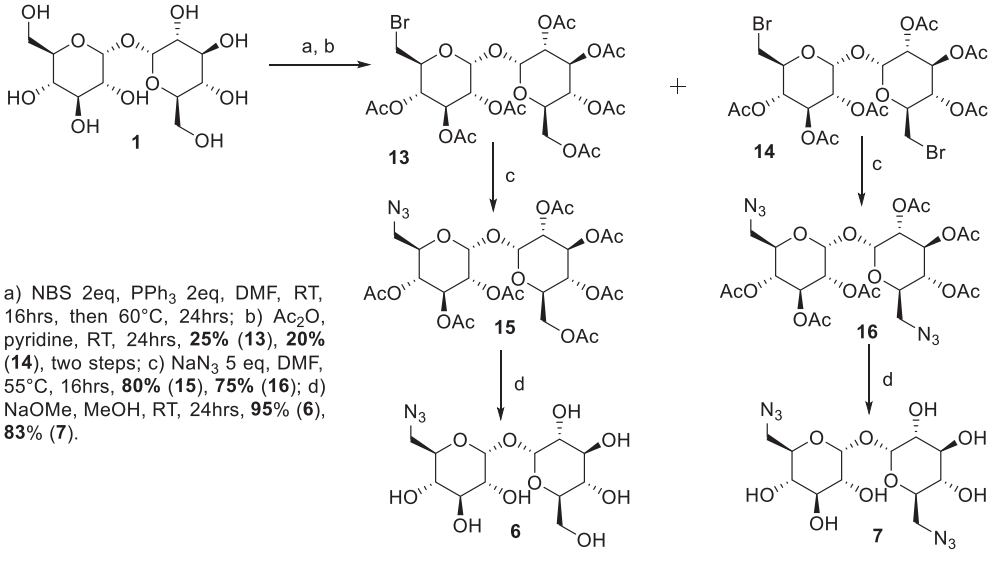

Scheme 1. Synthesis of 6-azido trehalose **6** and 6,6′-bisazido trehalose **7**.

Similarly, standard PEG-AuNPs **12b** were prepared by substituting trehalose conjugate **11** with PEG methyl ether thiol (average MW 800). TEM analysis confirmed their quality, so that both AuNPs **12a** and **12b** were submitted to biology profiling as putative autophagy inducers.

We initially profiled derivatives **2**–**10** and nanovectors **12a** in HeLa cells for their capability to induce autophagy. We monitored autophagy by tracking the mobility shift from LC3I to LC3II, that is a proxy for the induction of autophagy; and the amount of LC3II, that correlates with the number of autophagosomes[8]. We measured α -tubulin levels as an internal control in our assays. We treated HeLa cultures for 24 h at 37 °C with compounds **2**–**6** (2.5 mM), **7** (25, 50 μM), **8** (25, 50 μM), **9** (2.5 mM), **10** (200 μM, 2 mM), control vehicle (DMSO), and trehalose (100

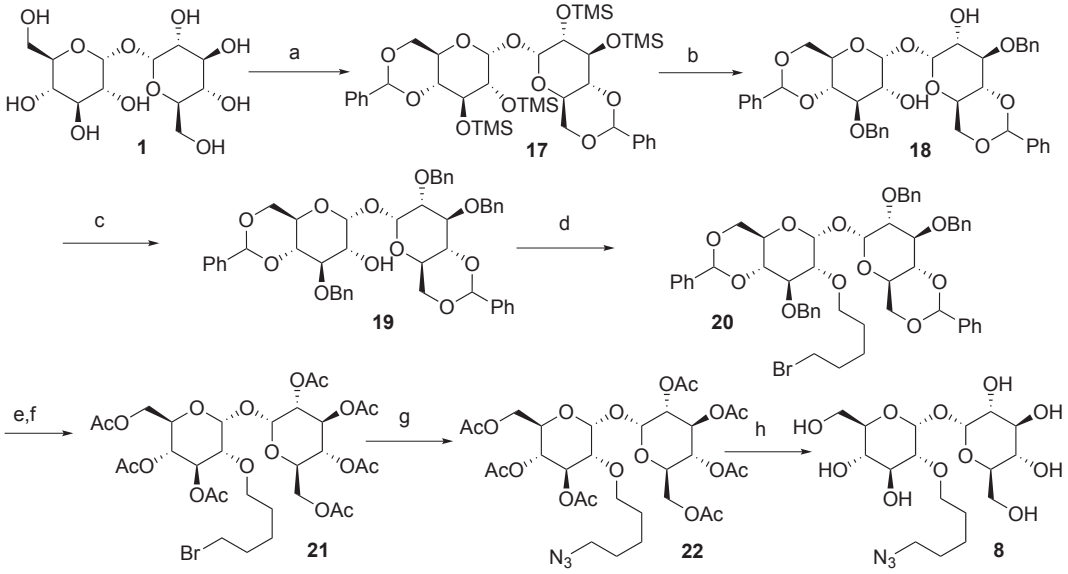

a) $PhCH(OMe)_2$ 2.2eq, cat PTSA, DMF, 105-100°C, 100min, then TMSCl, 1H-Imidazole, 0° to RT, 18hrs, **76%**; b) cat TMSOTf, PhCHO, Et_3SiH, DCM -78°C to 0°C, 6hrs, **80%**; c) BnBr 0.75eq, NaH, THF, 0°C to RT, 6hrs, **49%;** d) $Br(CH_2)_5Br$ 10eq, NaH 2eq, DMF, 55°C, 4hrs, **71%** e) H_2, Pd-C, MeOH/THF 4:1, RT, 24hrs; f) Ac_2O, cat DMAP, DCM/Py, RT, 4hrs, **71%** over two steps; g) NaN_3, DMF 65°C, 16hrs, **90%**; h) NaOMe, MeOH, RT, 24hrs, **96%**.

Scheme 2. Synthesis of 2-(5-azidopentyl) trehalose **8**.

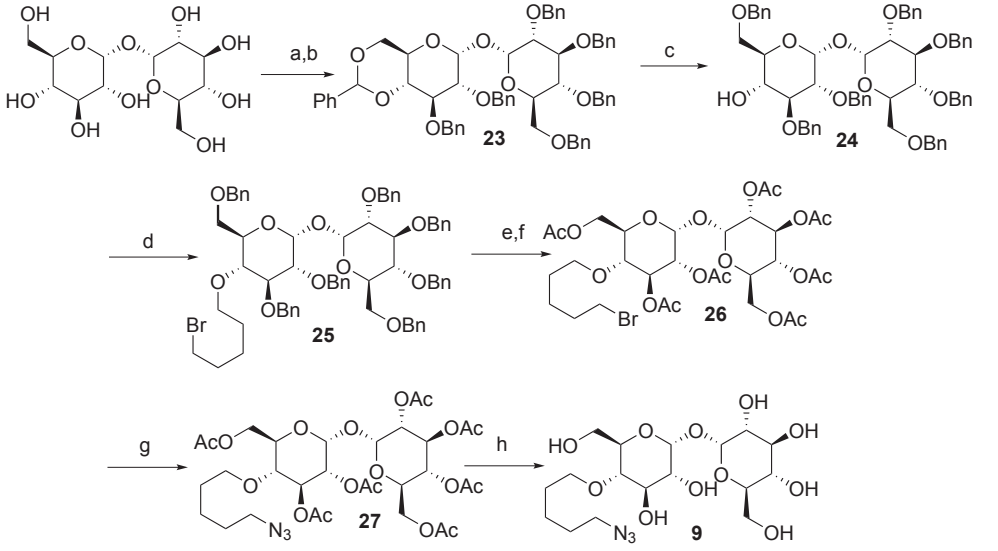

a) $PhCH(OMe)_2$ 1eq, PTSA 0.05eq, DMF, 105-100°C, 100min; b) BnBr 9eq, NaH 7.5eq, dry DMF, RT, 24hrs, **33%** over two steps; c) Et_3SiH 7.5eq, TFA 7.5eq, dry DCM, 0°C to RT, 4hrs, **78%**; d) $Br(CH_2)_5Br$ 10eq, NaH 2eq, DMF, 55°C, 4hrs, **70%;** e) H_2, Pd/C 10%, MeOH/THF 4:1, RT, 16hrs; f) Ac_2O, cat DMAP, DCM/Py, RT, 16hrs; g) NaN_3, DMF 65°C, 16hrs, **60%** over three steps; h) NaOMe, MeOH, RT, 8hrs, **98**%.

Scheme 3. Synthesis of 4(5-azidopentyl) trehalose **9**.

mM). Unfortunately, we did not appreciate any autophagic activation at the given experimental conditions for compounds **2**–**10** (Fig. 4).

We next evaluated the biological activity of PEG-AuNPs **12a** (diluted 1:400, 1:200, and 1:100 for an estimated, adjusted free-trehalose concentration around 10, 20, and 40 μM), of their non-assembled PEG-trehalose precursor **11** (10, 20, and 40 μM), of the PEG-linker (5, 10, 20 μM) and of the standard PEG-AuNPs **12b** (diluted 1:400, 1:200, and 1:100). Upon a 24 h long treatment, autophagy was not elicited by any sample at any concentration (Fig. 5).

Next, we repeated the assays after 48 h incubation to ensure the release of free trehalose from PEG-AuNPs **12a**; in these conditions, trehalose-bearing AuNPs **12a** efficiently induced autophagy and increased the number of autophagosome at the higher estimated concentration of free trehalose (40 μM, Fig. 6).

We verified the *in vitro* safety of trehalose-bearing AuNPs **12a** after 24 and 48 h incubation by a standard MTT cytotoxicity assay. They induced only limited cytotoxicity at the estimated free trehalose concentration of 40 μM upon 24 h treatment, but were well tolerated upon 48 h incubation (Fig. 7).

Bafilomycin A1 is an inhibitor of autophagosome-lysosome fusion *in*

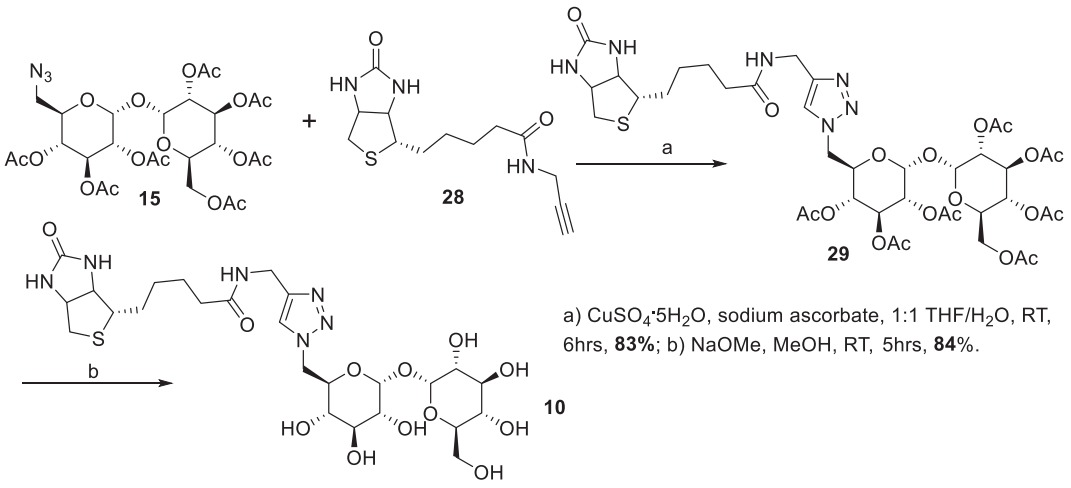

Scheme 4. Synthesis of biotin-based trehalose chemical probe **10**.

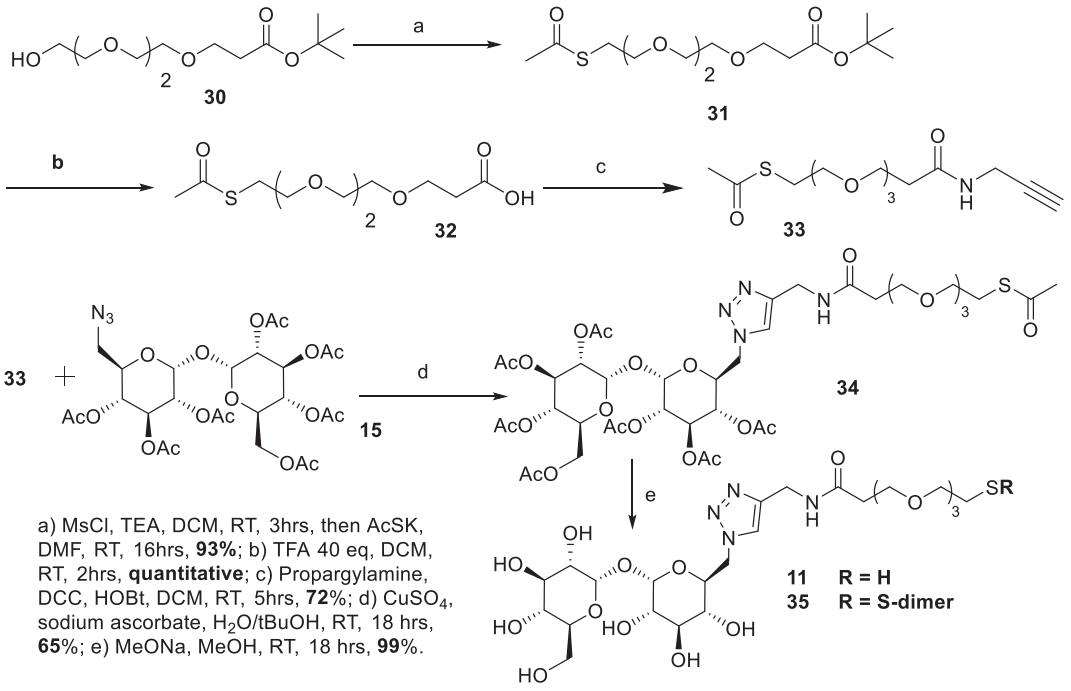

Scheme 5. Synthesis of thiol-PEG-triazole-trehalose adduct **11** for functionalization of inorganic nanovectors.

vitro and it enables to determine the activity of the autophagic flux. Thus, we treated cells with compound **1** (100 mM) and **12a (**40 μM) alone or in presence of bafilomycin 1A (10 nM) for 48 h, and we monitored the amount of LC3II (Fig. 8A). Remarkably, we noticed that bafilomycin 1A had a synergistic effect on both compound **1** and **12a** (Fig. 8B).

Our goal was to identify trehalose-based novel chemical entities with measurable autophagy-inducing properties, and to synthesize biologically active trehalose-based probes to gather information about its molecular mechanism of action. We reasoned that a small array made of prodrugs (**2**–**5**), putative probes (**6**–**10**) and inorganic nanovectors (**12a** as such, and the thiol-PEG-triazole-trehalose construct **11** used to build them) should have been enough to achieve our goals.

Acetylated trehalose derivatives **2**–**5** were earlier studied as intracellular delivery trehalose vehicles[26], with hexa-acetylated **4** showing increased membrane permeability. Unfortunately, we could not show an autophagy-inducing effect up to low mM concentrations for **2**–**5**, thus disproving their potential usefulness as bioavailable trehalose prodrugs.

Trehalose azides **6**–**9** and biotinylated trehalose **10** were designed respectively as putative photoactivatable probes[27] and as an affinity chromatography reagent[28]. If one among them would have shown significant activation of the autophagic flux, we would have either

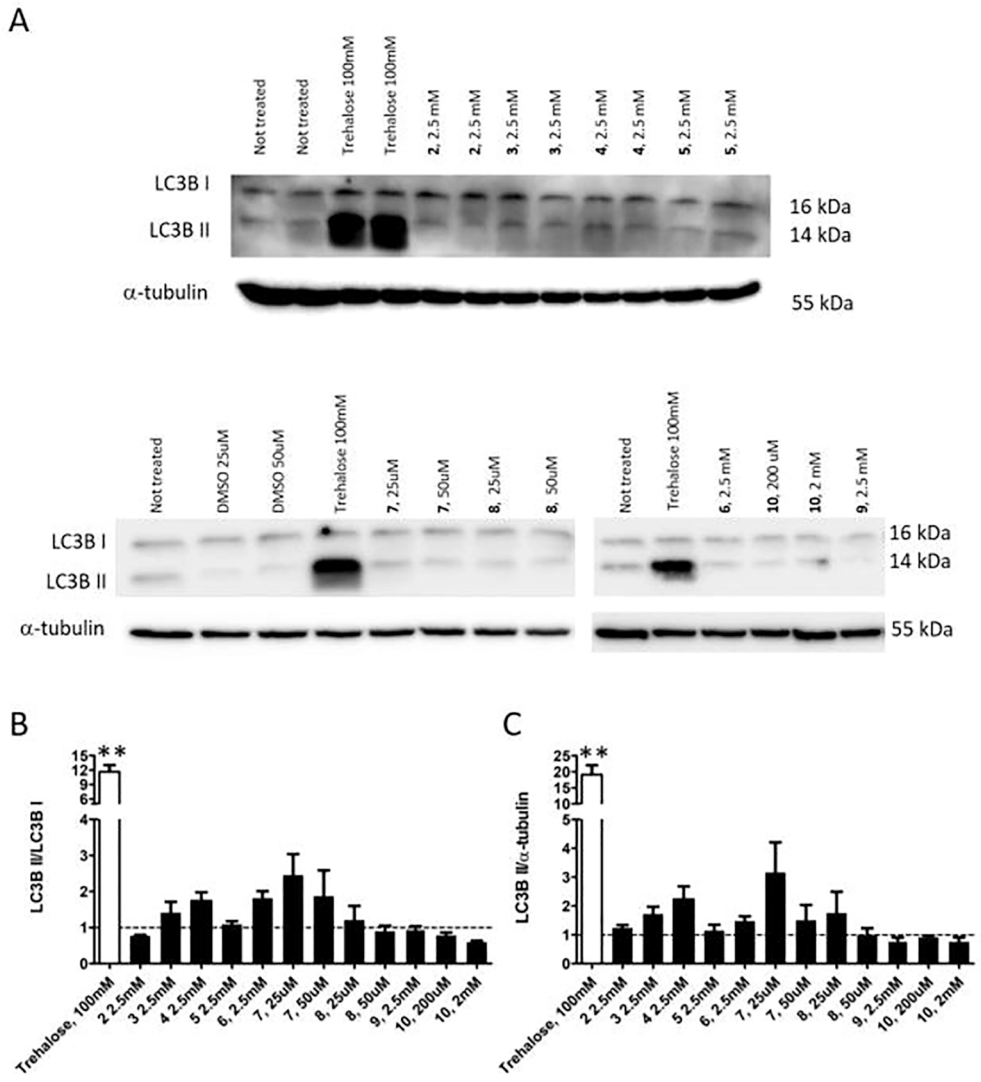

Fig. 4. Autophagy induction assay on compounds **2**–**10** upon 24 h treatment (A). Graphs report LC3BII/LC3BI ratio (B) and LC3BII amount expressed as fold over α -tubulin (C). Each value was normalized on proper control. Data are expressed as mean ± S.E.; n = 6–8, ** $p < 0.01$.

photoactivated it in cells showing autophagy stimulation, covalently binding to their unknown target either before or after cell lysis (**6**–**9**) or we would have incubated it in the same cells, whose lysates then were to be eluted on a streptavidin-coated support to identify the bound target (**10**). The lack of autophagy stimulation by trehalose analogues **6**–**10** prevented any mechanism of action-targeted experiment.

Such negative results suggest that any modification on trehalose hampers its biological activity. Instead, we considered that the identification of nanocarriers to improve trehalose pharmacokinetics properties may prove to be a convenient strategy. In a previous work we described trehalose-containing self-assembling NPs based on squalene[29], which did not influence the autophagic flux in our assays.

Conversely, we report here that trehalose-bearing AuNPs **12a** efficiently induce autophagy in cellular assays at a 40 μM estimated concentration, i.e. at a > 1000 lower concentration than the one needed for free trehalose to be active. We did not expect that AuNPs should modify the pharmacodynamic properties of trehalose. Rather, we are confident that the improved activity observed for compound **12a** stems from its improved pharmacokinetics properties, in particular stability and membrane permeability. Indeed, further studies will be performed to determine the bioavailability of compound **12a**.

Such results could have major therapeutic consequences and will be thoroughly exploited in the near future, up to in vivo testing in models of diseases showing autophagy disturbance.

Declaration of Competing Interest

The authors declare that they have no known competing financial interests or personal relationships that could have appeared to influence the work reported in this paper.

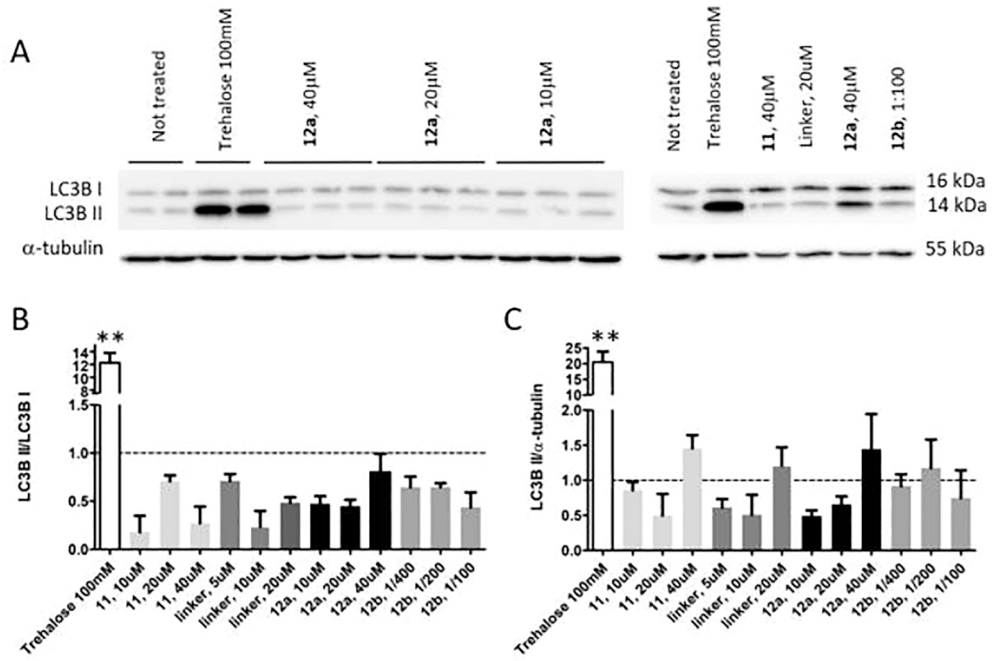

Fig. 5. Autophagy induction assay on conjugate **11**, PEG-linker, trehalose-bearing PEG-AuNPs **12a** and standard PEG-AuNPs **12b** upon 24 h treatment (A). Graphs report LC3BII/LC3BI ratio (B) and LC3BII amount expressed as fold over α-tubulin (C). Each value was normalized on untreated control. Data are expressed as mean ± S.E.; n = 6–8,** $p < 0.01$.

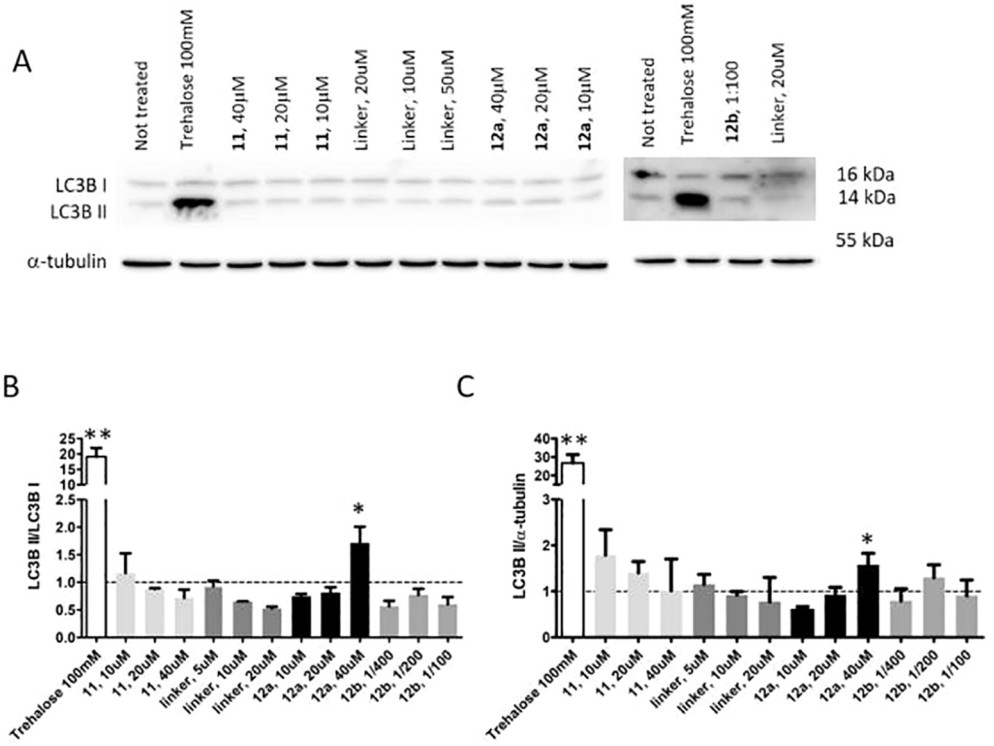

Fig. 6. Autophagy induction assay on conjugate **11**, PEG-linker, trehalose-bearing PEG-AuNPs **12a** and standard PEG-AuNPs **12b** upon 48 h treatment (A). Graphs report LC3BII/LC3BI ratio (B) and LC3BII amount expressed as fold over α-tubulin (C). Each value was normalized on untreated control. Data are expressed as mean ± S.E.; n = 6–8, * $p < 0.05$, ** $p < 0.01$.

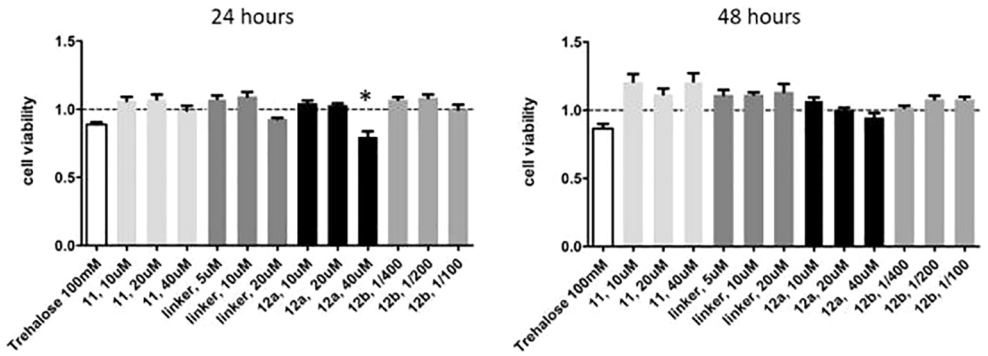

Fig. 7. MTT cytotoxicity assay on compound **11**, PEG linker, trehalose-bearing PEG-AuNPs **12a** and standard PEG-AuNPs **12b** upon 24 (left) and 48 h (right) treatments. Graphs report viability expressed as fold over control, set at 1. Data are expressed as mean ± S.E.; n = 6–8, * $p < 0.05$.

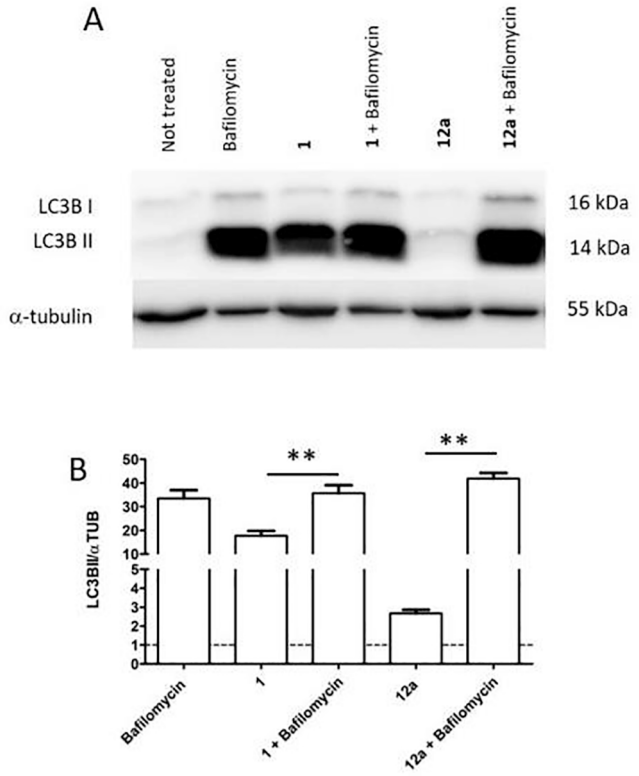

Fig. 8. Autophagy induction assay on trehalose **1** (100 mM) and PEG-AuNPs **12a** (40 mM) in presence of bafilomycin 1A (10 nM) upon 48 h treatment (A). The graph reports LC3BII amount expressed as fold over α-tubulin (B). Each value was normalized on not treated control, set at 1. Data are expressed as mean ± S.E.; n = 6–8, ** $p < 0.01$.

Acknowledgments

G.P. is supported by Fondazione Telethon (grant TDPG00514TA), MIUR (PRIN-2017ENN4FY), and Fondazione Cariplo (project 2019-3415).

Appendix A. Supplementary data

Supplementary data to this article can be found online at https://doi.org/10.1016/j.bmcl.2021.127929.

References

1 Birch GG. Trehaloses. *Adv Carbohydr Chem.* 1963;18:201–225. https://doi.org/10.1016/s0096-5332(08)60243-x.
2 Richards AB, Krakowka S, Dexter LB, et al. Trehalose: a review of properties, history of use and human tolerance, and results of multiple safety studies. *Food Chem Toxicol.* 2002;40(7):871–898. https://doi.org/10.1016/S0278-6915(02)00011-X.
3 Paiva CL, Panek AD. Biotechnological applications of the disaccharide trehalose. *Biotechnol Annu Rev.* 1996;2:293–314. https://doi.org/10.1016/s1387-2656(08)70015-2.
4 Van Dijck P, Colavizza D, Smet P, Thevelein JM. Differential importance of trehalose in stress resistance in fermenting and nonfermenting Saccharomyces cerevisiae cells. *Appl Environ Microbiol.* 1995;61(1):109–115. https://doi.org/10.1128/AEM.61.1.109-115.1995.
5 Komes D, Lovric T, Ganic KK, Gracin L. Study of trehalose addition on aroma retention in dehydrated strawberry puree. *Food Technol Biotechnol.* 2003;41:111–119.
6 Tanaka M, Machida Y, Niu S, et al. Trehalose alleviates polyglutamine-mediated pathology in a mouse model of Huntington disease. *Nat Med.* 2004;10(2):148–154. https://doi.org/10.1038/nm985.
7 Kalf GF, Rieder SV. The purification and properties of trehalase. *J Biol Chem.* 1958;230(2):691–698.
8 Chen X, Li M, Li L, et al. Trehalose, sucrose and raffinose are novel activators of autophagy in human keratinocytes through an mTOR-independent pathway. *Sci Rep.* 2016;6:28423. https://doi.org/10.1038/srep28423.
9 Mardones P, Rubinsztein DC, Hetz C. Mystery solved: Trehalose kickstarts autophagy by blocking glucose transport. *Sci Signal.* 2016;9(416). https://doi.org/10.1126/scisignal.aaf1937.
10 Rusmini P, Cortese K, Crippa V, et al. Trehalose induces autophagy via lysosomal-mediated TFEB activation in models of motoneuron degeneration. *Autophagy.* 2019;15(4):631–651. https://doi.org/10.1080/15548627.2018.1535292.
11 O'Neill MK, Piligian BF, Olson CD, Woodruff PJ, Swarts BM. Tailoring trehalose for biomedical and biotechnological applications. *Pure Appl Chem.* 2017;89(9):1223–1249. https://doi.org/10.1515/pac-2016-1025.
12 Iordachescu M, Imai R. Trehalose biosynthesis in response to abiotic stresses. *J Integr Plant Biol.* 2008;50(10):1223–1229. https://doi.org/10.1111/j.1744-7909.2008.00736.x.
13 Rodriguez Lavado J, Sestito SE, Cighetti R, et al. Trehalose- and glucose-derived glycoamphiphiles: small-molecule and nanoparticle Toll-like receptor 4 (TLR4) modulators. *J Med Chem.* 2014;57(21):9105–9123. https://doi.org/10.1021/jm501182w.
14 Wolber JM, Urbanek BL, Meints LM, et al. The trehalose-specific transporter LpqY-SugABC is required for antimicrobial and anti-biofilm activity of trehalose analogues in Mycobacterium smegmatis. *Carbohydr Res.* 2017;450:60–66. https://doi.org/10.1016/j.carres.2017.08.003.
15 Swarts BM, Holsclaw CM, Jewett JC, et al. Probing the mycobacterial trehalome with bioorthogonal chemistry. *J Am Chem Soc.* 2012;134(39):16123–16126. https://doi.org/10.1021/ja3062419.
16 Kobayashi K, Saito R, Udagawa K, et al. Synthesis of 6,6′-bis(*O*-4-arylethynylbenzoyl)-α, α-trehaloses and their utilization as fluorescent probes for cellular imaging. *Eur J Org Chem.* 2018;2018(26):3444–3453. https://doi.org/10.1002/ejoc.201800424.
17 Rajaram H, Palanivelu MK, Arumugam TV, et al. 'Click' assembly of glycoclusters and discovery of a trehalose analogue that retards Aβ40 aggregation and inhibits Aβ40-induced neurotoxicity. *Bioorg Med Chem Lett.* 2014;24(18):4523–4528. https://doi.org/10.1016/j.bmcl.2014.07.077.
18 Pradhan N, Shekhar S, Jana NR, Jana NR. Sugar-Terminated Nanoparticle Chaperones Are 10^2–10^5 Times Better Than Molecular Sugars in Inhibiting Protein Aggregation and Reducing Amyloidogenic Cytotoxicity [published correction appears in ACS Appl Mater Interfaces. 2019 Sep 4;11(35):32577]. *ACS Appl Mater Interfaces.* 2017;9(12):10554–10566. https://doi.org/10.1021/acsami.7b01886.
19 Mandal S, Debnath K, Jana NR, Jana NR. Trehalose-functionalized gold nanoparticle for inhibiting intracellular protein aggregation. *Langmuir.* 2017;33(49):13996–14003. https://doi.org/10.1021/acs.langmuir.7b02202.

20 Narouz M, Soliman S, Bassily R, El-Sokkary R, Nasr A, Nashed M. Improved synthesis of 6-azido-6-deoxy- and 6,6′-diazido-dideoxy- α, α-trehaloses. *Synlett*. 2013;24(17):2271–2273. https://doi.org/10.1055/s-0033-1339843.
21 Wang CC, Lee JC, Luo SY, et al. Synthesis of biologically potent alpha1–>2-linked disaccharide derivatives via regioselective one-pot protection-glycosylation. *Angew Chem Int Ed Engl*. 2002;41(13):2360–2362. https://doi.org/10.1002/1521-3773(20020703)41:13<2360::AID-ANIE2360>3.0.CO;2-R.
22 Dreaden EC, Alkilany AM, Huang X, Murphy CJ, El-Sayed MA. The golden age: gold nanoparticles for biomedicine. *Chem Soc Rev*. 2012;41(7):2740–2779. https://doi.org/10.1039/c1cs15237h.
23 Haume K, Rosa S, Grellet S, et al. Gold nanoparticles for cancer radiotherapy: a review. *Cancer Nanotechnol*. 2016;7(1). https://doi.org/10.1186/s12645-016-0021-x.
24 Boisselier E, Astruc D. Gold nanoparticles in nanomedicine: preparations, imaging, diagnostics, therapies and toxicity. *Chem Soc Rev*. 2009;38(6):1759–1782. https://doi.org/10.1039/b806051g.
25 Arosio D, Chiodo F, Reina JJ, et al. Effective targeting of DC-SIGN by α-fucosylamide functionalized gold nanoparticles. *Bioconjug Chem*. 2014;25(12):2244–2251. https://doi.org/10.1021/bc500467u.
26 Abazari A, Meimetis LG, Budin G, Bale SS, Weissleder R, Toner M. Engineered trehalose permeable to mammalian cells. *PLoS One*. 2015;10(6):e0130323. https://doi.org/10.1371/journal.pone.0130323.
27 Smith E, Collins I. Photoaffinity labeling in target- and binding-site identification. *Future Med Chem*. 2015;7(2):159–183. https://doi.org/10.4155/fmc.14.152.
28 Hage DS, Anguizola JA, Bi C, et al. Pharmaceutical and biomedical applications of affinity chromatography: recent trends and developments. *J Pharm Biomed Anal*. 2012;69:93–105. https://doi.org/10.1016/j.jpba.2012.01.004.
29 Colombo E, Biocotino M, Frapporti G, et al. Nanolipid-trehalose conjugates and nano-assemblies as putative autophagy inducers. *Pharmaceutics*. 2019;11(8):422. https://doi.org/10.3390/pharmaceutics11080422.